CENTRE DE RECERCA MATEMÀTICA

Preprint núm. 1215
October 2015

Memory and adaptive behaviour and in population dynamics: Anti-predator behaviour as a case study

A. Pimenov, T.C. Kelly, A. Korobeinikov, M.J.A. O'Callaghan, D. Rachinskii

MEMORY AND ADAPTIVE BEHAVIOUR AND IN POPULATION DYNAMICS: ANTI-PREDATOR BEHAVIOUR AS A CASE STUDY

ALEXANDER PIMENOV, THOMAS C. KELLY, ANDREI KOROBEINIKOV, MICHAEL J.A. O'CALLAGHAN, DMITRII RACHINSKII

Abstract. Memory enables to forecast future on the basis of experience, and thus, in some form, is principally important for development flexible adaptive behaviour by animal communities. To model memory, in this paper we use the concept of hysteresis, which mathematically is described by Preisach operator. As case study, we consider anti-predator adaptation in the classic Lotka-Volterra predator-prey model. Despite its simplicity, the model allows to naturally incorporate all essential features of an adaptive system and memory. Simulations show that a system with memory can have a continuum of equilibrium states.

1. Introduction

Motivation. The ability to adapt to changing conditions is an essential feature of life and a key for its survival and reproductive success, and memory, which enables to forecast future on the basis of experience, is a vital component of the mechanism of adaptation. Memory, in some form, appears to be inherent for life. "Implicit memory", classified into short-, medium- and long-term forms, was found among heterotrophic eukaryotes, e.g., mollusks and insects [1, 2]. A map-like spatial memory is used in visual navigation by insects, such as bees and ants [3, 4]. Explicit, or declarative memory, which characterizes sentient man, most likely evolved from the ancestral implicit state [1]. However, there is mounting evidence that a sophisticated "episodic-like" memory is possessed by some birds, e.g., crows (*Corvidae*) [5, 6, 7], which enables them to remember "when, where and what" in relation to past events, to plan for the future, and in effect to engage in mental time travel — a property previously thought to be associated exclusively with *Homo sapiens* [8]. Apparently, the ability to memorize past events and then forecast and plan for the future should have a lasting impact on human or animal behaviour. Our objective is to explore the impact that past experience of individuals may have on population dynamics when such experience becomes a factor of their adaptive strategies.

Key words and phrases. Memory, Preisach operator, hysteresis, adaptation, predator-prey model, refuge.

CRM Preprint Series number 1215

As a convenient setting for this study we choose the predator-prey formalism, where we include the adaptive response of the prey to the pressure of predation. Although the Lotka-Volterra model, which we use as the case study, is not the only possible application for illustrating our approach, it allows us to straightforwardly include the "cost of safety" factor that is naturally incurred by adaptation strategies. This model is also convenient, because we can easily compare its outcomes in the case of adaptive response based on memory of the past with the case of the memoryless adaptive response that we have recently studied in [9]. Thus, we consider a predator-prey system where the prey has an immediate access to a refuge in a broad sense: it can either be a physical refuge, where the prey hides (as, for example, in [10, 11, 12, 13, 14]), or an anti-predator behaviour which is safer compared to that of the prey in a predator free environment (which, in contrast, we call *risky*). As the limiting case for this scenario one could consider a situation on islands where predators are sometimes completely absent [15], see also [16]. We model the ability of prey to adapt to external conditions by allowing an individual animal at any instance of time to choose either a "safe" mode of behaviour, or a "risky" behaviour. The choice is governed both by (i) current perceived level of threat imposed by the predator, and (ii) level of threat experienced by the prey animal in the past (some form of memory). To formulate a model of memory-based adaptive response, we adopt the general approach proposed in [17], which is related to the paradigm of hysteretic memory.

Modelling memory. In order to keep the model as simple as possible, we prefer to avoid assumptions where an individual prey animal adopts a particular mode of behaviour on the basis of some complex rule that would use any form of detailed information of the history. Instead, for simplicity, we use a basic model known as bi-stability or elementary hysteresis, where an individual switches from risky to safe mode of behaviour when the perceived level of threat exceeds a certain threshold value α_S and switches back from the safe to the risky mode of behaviour when the level of threat drops below a different (lower) threshold value α_R. The case when the switching thresholds coincide, $\alpha_R = \alpha_S$, corresponds to the memoryless adaptation strategy that has been considered in [9] and will be used here as a reference. In the hysteretic case, $\alpha_S > \alpha_R$, whenever the level of threat lies between the thresholds α_R and α_S (that is, within the bi-stability interval) the actual mode of behaviour adopted at this moment is a simple function of the past (risky, if the last threshold crossing was at α_R, and safe if the last threshold crossing was at α_S).

Although the above hysteresis-based model of individual adaptation strategies, known as the bi-stable switch or non-ideal relay, is simple, a quite complex memory of the past emerges at the level of the whole prey population, if we take into account that the threshold values vary among the individuals. At any moment in time, the prey population is distributed over two states (risky and safe), and this distribution, that varies with time, records (depends upon) many features of

CRM Preprint Series number 1215

the population dynamics history. In particular, this distribution is affected by a sequence of maximal and minimal levels of threat experienced by the prey in the past. This emerging complex memory can be described using the formalism of the classical Preisach model, which is a cornerstone of the modern mathematical theory of hysteresis operators (see [62] and bibliography therein).

Hysteresis vs alternative models of memory. Differential equations with delays provide a traditional apparatus for mathematical modelling of memory effects in biology. However, delayed equations, as well as other linear tools such as convolution integrals, impose an explicit time scale onto the memory deletion process. That is, either the evolution is determined by the past states of the system achieved a given time ago, as in the case of discrete delays, or the effect of the past states on the future decays (typically, exponentially) at a given rate. This contrasts to the hysteresis-based memory of the bi-stable switch, often called a permanent or rate-independent memory, because the effect of the past on the future is not limited to any a priori prescribed interval of time. Indeed, suppose, for example, that the input (the level of threat) temporarily increases from a value α lying within the bi-stability range (α_R, α_S) to some value exceeding the upper threshold α_S and then returns to the initial level alpha. A bi-stable switch that initially was in state "risky" will respond to this temporary increase of the input by switching to state "safe" where it will reside afterwards as long as the input will remain above the lower threshold α_R. This behaviour can be interpreted as permanent memory of a temporary variation of the input, because the "safe" state of the switch continues to record the input variation for unlimited time even after the applied stimulus has been removed (the input is returned to its initial value α and is kept at this value afterwards). This memory can be erased in the future only by another stimulus that brings the input value below the threshold α_R thus resulting in a transition of the switch back to the "risky" state.

Of course, hysteresis based permanent memory is an idealization, but it is a useful one if the characteristic time for which the prey retains the memory of its past experience (that the memory affects its choice of the adaptation strategy) is much longer than a typical time interval between substantial variations of the level of threat from the predator that cause the prey to change its behaviour. This consideration related to characteristic time scales is typical and can be compared to the situation in magnetic recording technologies, an area where the Preisach model has been massively employed. The lifetime of a magnetic record is limited by thermal fluctuations that cause the bi-stable magnetic particles to randomly switch the orientation of their magnetic moment. The Preisach model of a permanent magnet works well on time intervals that are shorter than a typical time scale set by the thermal memory deletion process.

Under the above limitation, the hysteresis based memory model can have an advantage over models employing delays, as hysteresis is not associated with any explicit time scale of the memory deletion process, which might be inadequate

CRM Preprint Series number 1215

and is hardly measurable. We will further discuss the relevance of hysteresis to the development of defensive responses and optimization of the survival strategy as well as the factors of fear and herding behaviour in the Conclusions section.

The cost of safety. A preliminary advance in applying hysteresis and the Preisach operator formalism to modelling biological systems with memory was done in [17, 18]. In these papers, the concept of dynamical memory effect called Permanent Effects of a Temporary Stimulos (PETS) was introduced and the impacts of PETS were studied for a specific problem of the spread of an infectious disease in a population. A basic Susceptible-Infectious-Recovered (SIR) epidemic model was employed as a convenient case study.

The model, considered in [17, 18], exhibits remarkable qualitative effects. In particular, a continuum of equilibrium states is possible for this model, and the convergence to a particular equilibrium state depends on the system pre-history. However, this model is not suitable for analysis of adaptive behaviour, as it assumes no cost for the safe behaviour. As a result, for this model the advantageous (safe) behaviour does not involve any explicit disadvantages, and hence there is no apparent reason for an individual to switch to disadvantageous and endangering behaviour again. The reason for this deficiency is that instituting explicit costs into the frameworks of a SIR model is hardly feasible. Instead, the model includes a sort of underlying understanding that there is a certain cost associated with the safe behaviour (for instance, it can be merely inconvenience induced by the need to behave safely), and hence an individual tends to return to "business as usual" mode (risky behaviour). However, the lack of explicitly incorporated costs of advantageous behaviour still should be considered as a shortcoming.

In order to close this gap and explore the effect of memory based adaptive response on dynamics of populations, we choose a different modelling framework. A predator-prey model is convenient for our objectives because it allows a straightforward institution of both the idea of adaptation of behaviour and the concept of the safety cost. For a population model, such as the predator-prey model that we consider, this cost can be naturally instituted in the terms of reproduction abilities, or reproduction rate. In other words, for such a model it is reasonable to assume that safety is paid for by either a direct reduction of reproduction, or an indirect reduction caused by a reduced access to a resource (food) [19, 20]. We leave the detail of how the safety can be achieved out of our consideration; some relevant discussion can be found in [9] and in the literature cited therein. The most obvious methods which increase the safety are using a refuge, forming defensive groups, or simply spending time and effort for monitoring the surrounding area. The associated reduction of the reproduction rate can be caused by avoiding rewarding but dangerous feeding or breeding grounds, or spending energy for defence.

The ability of animals to reduce the risk of predator attacks by modifying their behaviour, as well as the fact that the secure behaviour must incur certain

CRM Preprint Series number 1215

disadvantages, was long recognised and confirmed by observations and experiments (e.g., see [13, 14]). Mathematical models developed for a few particular cases revealed a number of phenomena caused by adaptive behaviour. In particular, the model constructed by [13] demonstrates the Allee effect caused by adaptive response of the prey rather than by community effects in the predator population. However, these models, as well as many other models (e.g., [Hendrison, the check]), were formulated as ordinary differential systems and neither of these assumed any kind of memory. A systematic institution of the adaptive (memoryless) prey behaviour was done in [9], where two modes of behaviour were postulated, and it was assumed that an individual switches from one to another mode when a value of a certain stimulus (level of threat) reaches an individual threshold level. It was assumed that the stimulus is proportional to a probability for an individual to be attacked and that the switching thresholds are individual and distributed in the population with a given distribution. This ordinary differential model with incorporated safety cost demonstrated that a coexistence of two stable positive equilibrium states, separated by a separatrix of a saddle point, is possible in such a predator-prey system. In this paper, we modify this model by including hysteresis based memory in the adaptive response using the formalism developed in [17]. Namely, we just need to postulate two different thresholds for each individual prey, one associated with switching the risky mode of behaviour to the safe mode and the other for the opposite switching.

The initial premise for our study is that in a situation when the risk of predator attack is high, it can be advantageous for the prey to adopt a safe mode of behaviour accepting the cost it incurs, whereas when the predation is low, an advantage can be gained exploiting richer feeding grounds. We note that for a predator-prey model, the Darwinian fitness of the prey is the ratio of the current reproduction rate to the attack rate. It is easy to see that the above-mentioned adaptive strategy increases only a relative fitness. One should take in consideration that if there is a strategy that increases the absolute rather than a relative fitness, than a group or a subspecies adopting this strategy would overcompete the rest of the population and eventually it would be the only type present, and no further changes of behaviour would be then feasible.

The paper is structured as follows. In the next section, we present our modeling approach. Section 3 contains analysis of branches of equilibrium points and numerical results that characterise their stability. Conclusions are presented in the last section.

2. Model

2.1. **Colouring approach.** We divide the environment into cells of equal size/volume that corresponds to the volume which a prey can grasp using its sensory systems. Inside each cell prey can exhibit *risky* or *safe* mode of behaviour. In the risky mode the prey is more vulnerable to the predator, whereas

CRM Preprint Series number 1215

in the safe mode it is subject to stronger competition and lower food availability. We begin with the simplifying assumption of *coloured* cells.

Assumption 1 (Coloured cell)**.** *At any given moment in time, all the prey in any given cell is in the same mode of behaviour.*

This assumption is natural if the prey "*colours*" the cell by using a defensive mechanism, taking collective actions, or changing its local habitat properties, when it switches from the risky to safe mode and from the safe to risky mode. We will show later that an equivalent assumption can be justified when a refuge patch is available for the prey. The birth, competition, and attack rates for prey in the risky mode are b_R, c_R, a_R, respectively; for the safe mode, they are b_S, c_S, a_S, where $a_R \geq a_S, b_R \geq b_S, c_R \leq c_S$. With this notation, the time evolution of the total number of prey $u = u(t, \mathbf{x})$ in a cell $\mathbf{x}$ is assumed to be defined by the equation

$$\dot{u} = b_i u - c_i u^2 - a_i uv$$

where $i = R$ when the prey is in the risky mode; $i = S$ when the prey is in the safe mode; v is the total number of predator; and, dot denotes the derivative with respect to time.

Assumption 2 (Heterogeneity)**.** *At a given moment in time, prey can have different mode of behaviour in different cells.*

Heterogeneity in prey's behaviour may result from a heterogeneity of the habitat.

Assumption 3 (Stimuli: reaction to predator)**.** *Prey in a cell* $\mathbf{x}$ *switches between the safe and risky modes of behaviour in response to stimuli* $A(t)$*. We assume that* A *is a function of the number of predators* v*.*

We will describe the prey's mode of behaviour by the binary function of time $(R_{\mathbf{x}}A)(t)$ which equals 0 when the prey is in the risky mode and 1 when the prey is in the safe mode. Here $R_{\mathbf{x}}$ is a an operator that maps the time series of stimuli $A(t)$ to this binary function of time. Hence, the rate equations for the number of prey can be combined to the equation

$$\dot{u}=(b_R(1-R_{\mathbf{x}}A)+b_S R_{\mathbf{x}}A)u-(c_R(1-R_{\mathbf{x}}A)+c_S R_{\mathbf{x}}A)u^2-(a_R(1-R_{\mathbf{x}}A)+a_S R_{\mathbf{x}}A)uv.$$

The simplest option is to assume that $R = R_{\alpha_S}$ is an *ideal relay* (the shifted Heaviside step function)

$$R_{\alpha_S}(A) = \begin{cases} 0, & \alpha_S \geq A, \\ 1, & \alpha_S < A, \end{cases} \tag{1}$$

where the value of the switching threshold $\alpha_S = \alpha_S(\mathbf{x})$ is individual to a cell $\mathbf{x}$, and is defined by the cell's properties and the ability of prey to perceive the

stimuli in this cell. Then the rates $r = a, b, c$ switch between the safe and risky values according to the formula

$$r = r_S R_{\alpha_S(\mathbf{x})}(A) + r_R(1 - R_{\alpha_S(\mathbf{x})}(A)).$$

However, this switching strategy is memoryless and does not lead to a hysteretic behaviour. Instead, we assume a more complex response of the prey to the stimuli.

Assumption 4 (Feedback: reaction to other prey)**.** *Reaction of the prey to the stimuli $A(t)$ is enhanced by a positive feedback loop coupled with the ideal relay response* (1) *and resulting in the existence of two switching thresholds. The prey switches the risky mode of behaviour to the safe mode when the stimuli $A(t)$ increase above a threshold value α_S; it switches back to the risky mode when the stimuli drop below a lower threshold value $\alpha_R < \alpha_S$. The switching threshold values $\alpha_S(\mathbf{x})$, $\alpha_R(\mathbf{x})$ are a property of a cell and vary from cell to cell.*

The positive feedback may result from the herding behavior of the prey. Herding describes the situation where the fact that other prey is in the safe mode acts as an additional stimulus for a prey species to stay in the safe mode, effectively pushing the switching threshold of the response to the variation of the predator-controlled stimuli $A(t)$ from the value α_S adopted by the prey when in the risky mode to a lower value α_R when in the safe mode. According to Assumption 4, the time series of stimuli $A(t)$, where $t \geq t_0$, is mapped to the binary time series of the mode of prey's behaviour by the so-called *non-ideal relay* relay operator [21]

$$(2) \qquad (R_{\alpha_R,\alpha_S}[\eta(t_0)]A)(t) = \begin{cases} 0 & \text{if} \quad A(\tau) \leq \alpha_R \text{ for some } \tau \in [t_0, t] \\ & \quad \text{and } A(s) < \alpha_S \text{ for all } s \in [\tau, t]; \\ 1 & \text{if} \quad A(\tau) \geq \alpha_S \text{ for some } \tau \in [t_0, t] \\ & \quad \text{and } A(s) > \alpha_R \text{ for all } s \in [\tau, t]; \\ \eta(t_0) & \text{if} \quad \alpha_R < A(\tau) < \alpha_S \text{ for all } \tau \in [t_0, t], \end{cases}$$

where $\eta(t_0)$ is the state (mode of behaviour) of the prey at the initial moment t_0, that is either $\eta(t_0) = 0$, or $\eta(t_0) = 1$. The non-ideal relay (2) can indeed be obtained as the solution operator of the equations $y(t) = (R_{\alpha_S}x)(t)$, $x(t) = A(t) + y(t)\Delta$ describing the system, which consists of the ideal relay (1) with the input $A(t)$ and a positive feedback loop. The coefficient Δ controlling the feedback strength defines the difference $\Delta = \alpha_S - \alpha_R$ of thresholds of the non-ideal relay. Assumption 4 implies that the dependence of the attack, birth and competition rates $r = a, b, c$ on the varying stimuli $A(t)$ is described by the relationship

$$(3) \qquad r_{\alpha_R(\mathbf{x}),\alpha_S(\mathbf{x})} = r_S R_{\alpha_R(\mathbf{x}),\alpha_S(\mathbf{x})}[\eta(t_0)]A + r_R(1 - R_{\alpha_R(\mathbf{x}),\alpha_S(\mathbf{x})}[\eta(t_0)]A).$$

The non-ideal relay is the most basic, yet non-trivial, example of a hysteretic input-state relationship. If $A(t) \geq \alpha_S$ at some moment t, then the state $\eta(t) = (R_{\alpha_R,\alpha_S}[\eta(t_0)]A)(t)$ of the relay at the same moment is 1; if $A(t) \leq \alpha_R$, then

$\eta(t) = 0$. However, the switching rules (2) are defined in such a way that when the current value of the input falls within the interval $\alpha_R < A(t) < \alpha_S$ between the switching thresholds, then the simultaneous value of the state $\eta(t)$ of the relay depends on the input history prior to the moment t. The most important property of memory in the input-state relationship of the non-ideal relay, as well as other models of hysteresis, is *rate-independence*. The rate-independence means the state does not depend on the rate at which the input may have varied, but rather on the past values of the input extrema. This is an important form of memory that persists on a long time scale and can not be attained by linear dynamic systems whose memory is typically associated with certain characteristic times, rather than input features such as extrema. Hysteresis and multi-stability, with the associated memory, have been demonstrated in many different biological contexts.

Having discussed prey in an individual cell, we proceed to the whole ensemble of the cells.

Assumption 5 (Heterogeneity of switching thresholds)**.** *The threshold values $\alpha_R(\mathbf{x}), \alpha_S(\mathbf{x})$ are distributed among all cells with a density $\mu(\alpha_R, \alpha_S)$.*

The last assumption concerns the movement of prey between the cells.

Assumption 6 (Free movement)**.** *Prey and predator move freely between and inside the cells according to a conventional diffusive process. The rate of diffusion is much higher than the rate of population processes.*

Due to fast diffusion, on the slow time scale of the population processes, the prey density and the predator density are uniform in space. That is, Assumption 6 allows us to average the system over the spatial variable $\mathbf{x}$. For example, assuming the ideal relay response (1) of prey ($\alpha_R = \alpha_S$ in Assumption 4) and a distribution of the switching threshold with the density function $\mu(\alpha_S)$, the average rates $\bar{r} = \bar{a}, \bar{b}, \bar{c}$ are

$$\bar{r} = \int_0^\infty (r_S R_{\alpha_S}(A) + r_R(1 - R_{\alpha_S}(A)))\mu(\alpha_S)d\alpha_S = r_S P_S(A) + r_R(1 - P_S(A)),$$

where $P_S(A)$ is the anti-predator functional response of the prey,

$$P_S(A) = \int_0^A \mu(\alpha)d\alpha$$

satisfying $0 \le P_S \le 1$. To obtain type I functional response, we can assume $A = \kappa v$ and

$$\mu(\alpha) = \begin{cases} 1, & \alpha \le 1, \\ 0, & \alpha > 1. \end{cases}$$

CRM Preprint Series number 1215

Then, under the assumption that $\kappa v \leq 1$, we obtain the following dynamical model of a predator and a two-mode prey populations:

$$\dot{u} = (b_S\kappa v + b_R(1-\kappa v))u - (c_S\kappa v + c_R(1-\kappa v))u^2$$

$$-(a_S\kappa v + a_R(1-\kappa v))vu, \tag{4}$$

$$\dot{v} = -dv + e(a_S\kappa v + a_R(1-\kappa v))vu, \tag{5}$$

where the proportions κv and $1-\kappa v$ of the prey population in the safe and risky modes of behaviour, respectively, are defined by the simultaneous number of predator v. By rearranging the terms, we arrive at a Lotka-Volterra model with non-standard functional response $F(u,v)$ and numerical response $N(u,v)$:

$$\dot{u} = b_R u - c_R u^2 - F(u,v), \qquad \dot{v} = -dv + N(u,v), \tag{6}$$

$$N(u,v) = ((a_S - a_R)\kappa v + a_R)vu, \tag{7}$$

$$F(u,v) = (D(u,v) - T(u,v))uv, \tag{8}$$

$$T(u,v) = \kappa(a_R - a_S)v \geq 0, \tag{9}$$

$$D(u,v) = a_R + \kappa(b_R - b_S) + \kappa(c_S - c_R)u \geq 0, \tag{10}$$

where $D(u,v)$ is the loss component due to predation and $T(u,v)$ represents the advantage of the anti-predator response. This system is close to the model studied in [14] where the proportion of prey in a refuge was defined by the number of predators. A similar model with two patches, including a rate equation for the prey population in each patch and assuming that the rate of flow of the prey to the refuge patch is controlled by the number of predator, was studied in [13].

Now, we assume the hysteretic response of prey to stimuli, which is defined by the non-ideal relay operator (2). In this case, the feedback loop introduced through herding ensures that any new prey arriving to a cell $\mathbf{x}$ due to the diffusion process adopts immediately the same mode of behaviour as the other prey populating this sell, thus providing for Assumptions 1 and 4 (with $\alpha_R < \alpha_S$). Hence, the averaged rate of population processes at a moment t is obtained by integrating the expression (3) for the rates with the weighting function $\mu(\alpha_R, \alpha_S)$:

$$\bar{r}(t) = \int_0^\infty \int_0^{\alpha_S} \mu(\alpha_R,\alpha_S) r_{\alpha_R,\alpha_S}(t)\, d\alpha_R d\alpha_S = r_S P_S(t) + r_R(1 - P_S(t)). \tag{11}$$

Here the time series of the anti-predator response of the prey $P_S(t)$, satisfying $0 \leq P_S(t) \leq 1$ at all times, is defined by the hysteretic operator

$$P_S(t) = \int_0^\infty \int_0^{\alpha_S} \mu(\alpha_R,\alpha_S)(R_{\alpha_R,\alpha_S}[\eta_0(\alpha_R,\alpha_S)]A)(t)\, d\alpha_R d\alpha_S =: (\mathcal{P}[\eta_0]A)(t), \tag{12}$$

which can be viewed as superposition of non-ideal relay operators with different thresholds. This operator $\mathcal{P} = \mathcal{P}[\eta_0]$, mapping the time series $A(t)$ to the time series $P_S(t)$, is known as the *Preisach operator* [21, 22]. The binary function $\eta_0 = \eta_0(\alpha_R, \alpha_S)$ in its definition is known as the initial state of the Preisach

CRM Preprint Series number 1215

operator; it describes the states of all the non-ideal relays at the initial moment. The time series $P_S(t)$ is a continuous function of time. The weighting function μ satisfies the condition $\int_0^\infty \int_0^{\alpha_S} \mu(\alpha_R, \alpha_S)\, d\alpha_R d\alpha_S = 1$.

Using Eq. (11) for the rates of population processes and assuming that the stimuli are proportional to the abundance of the predator, $A = \kappa v$, we obtain the following extension of model (6) – (10):

$$\dot{u} = (b_S P_S(t) + b_R(1 - P_S(t)))u - (c_S P_S(t) + c_R(1 - P_S(t)))u^2$$

$$-(a_S P_S(t) + a_R(1 - P_S(t)))vu, \tag{13}$$

$$\dot{v} = -dv + e(a_S P_S(t) + a_R(1 - P_S(t)))vu, \tag{14}$$

$$P_S(t) = (\mathcal{P}[\eta_0]y)(t), \qquad y(t) = \kappa v(t). \tag{15}$$

where $P_S(t)$ is the proportion of prey in the safe mode of behaviour; the operator $\mathcal{P}$ in Eq. (13) accounts for hysteresis (memory) in the response of the prey to the predator abundance, and $y(t)$ is the stimulus function.

As the simplest density function μ in Eq. (11), we will consider the function

$$\mu(\alpha_R, \alpha_S) = \begin{cases} 2, & 0 \le \alpha_R \le \alpha_S \le 1, \\ 0, & \text{otherwise}, \end{cases} \tag{16}$$

which generates the uniform distribution of switching thresholds in a unit triangle.

If the ideal relays are used instead of non-ideal relays, then the density function (16) corresponds to

$$\mu(\alpha) = \int_0^\alpha \mu(\alpha_R, \alpha) d\alpha_R = \begin{cases} 2\alpha, & \alpha \le 1, \\ 0, & \text{otherwise}, \end{cases}$$

and we obtain $P_S(t) = (\kappa v(t))^2$ rather than $P_S(t) = \kappa v(t)$ as discussed earlier in this section. The square dependence manifests the learning curve.

2.2. **Refuge analogy: repelling patches.** In this subsection, we show how a refuge analogy can produce a *coloured* cell according to Assumption 1. A cell is supposed to be composed of three patches: a neutral (intermediate) patch of volume ω_0, a free (risky) patch of volume ω_R, and a refuge (safe) patch of volume ω_S, see Fig. 1 (a). The population rates a_i, b_i, c_i in the patches ω_i satisfy $a_S \le a_0 \le a_R$, $b_S \le b_0 \le b_R$, and $c_R \le c_0 \le c_S$[1]. We assume that the refuge patch is repelling and the free patch is attractive for the prey in the risky mode of behaviour; whereas the refuge patch becomes attractive and the free patch becomes repelling for the scared prey. The neutral patch is always acceptable for the prey. The fast mixing Assumption 6 holds for the whole environment except repelling areas in the cells, where there is no prey. That is, at any given moment, the density of the predator is the same in all the patches of all the cells; the density of the prey is the same in the neutral and attracting patches of all the cells and zero in all the repelling patches.

[1]The neutral patch ω_0 may play the role of a transport route.

CRM Preprint Series number 1215

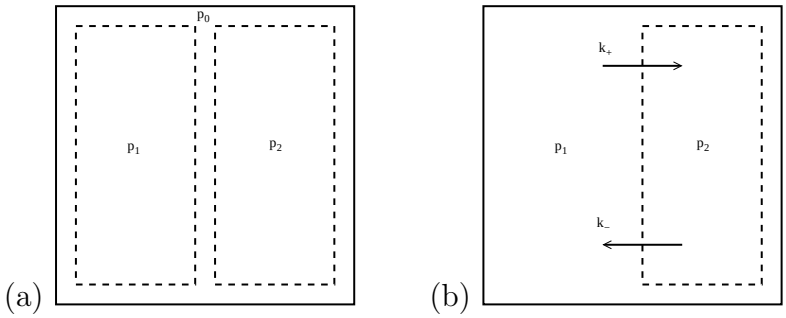

FIGURE 1. (a) Cell composition under the repelling patches assumption. In the risky mode of behaviour, refuge patch is repelling, free patch is attractive, intermediate patch is neutral. In the safe mode of behaviour, free patch is repelling, whereas refuge patch is attractive. In the neutral and attractive patches fast mixing Assumption 6 holds, and there is no prey in the repelling patch. (b) Cell composition in flow assumptions. In each mode of behaviour, there is a flow with constant rate k_+ from the free (risky) patch to the refuge (safe) patch and a flow in the opposite direction with the rate k_-, and fast mixing Assumption 6 holds inside both patches.

With the increase of stimuli $A(t)$ beyond the threshold value $\alpha_S = \alpha_S(\mathbf{x})$, the prey vacates the risky patch and populates the safe refuge patch in the cell $\mathbf{x}$; this may result in a change of prey's density (which happens on the fast time scale), as the total volume occupied by the prey changes if $\omega_R \neq \omega_S$. Due to the positive feedback loop (Assumption 4), the refuge patch remains occupied and the risky patch remains prey-free as long as $A(t) \geq \alpha_R$ with $\alpha_R < \alpha_S$. Applying Assumptions 5 and 6, we obtain the expression

$$\bar{r} = \frac{r_0\omega_0 + r_R\omega_R + (r_S\omega_S - r_R\omega_R)P_S(t)}{\omega_0 + \omega_R + (\omega_S - \omega_R)P_S(t)} \tag{17}$$

for the average attack and birth rates $r = a, b$; and the formula

$$\bar{c} = \frac{c_0\omega_0 + c_R\omega_R + (c_S\omega_S - c_R\omega_R)P_S(t)}{(\omega_0 + \omega_R + (\omega_S - \omega_R)P_S(t))^2} \tag{18}$$

for the average competition rate.

If $\omega_S = \omega_R$, then the volume occupied by the prey in each cell and the total volume of the habitat are constant at all times. If, in addition, $\omega_0 = 0$, then, using the same assumptions as in the previous subsection, we obtain exactly system (13) – (15). The relation $\omega_0 > 0$ results in extra linear terms in the system.

CRM Preprint Series number 1215

The case $\omega_S \neq \omega_R$ leads to an extension of model (13) – (15) where the first two equations are replaced by the equations

$$\begin{aligned} \dot{u} &= \bar{b}u - \bar{a}uv - \bar{c}u^2, \\ \dot{v} &= -dv + e\bar{a}uv \end{aligned} \tag{19}$$

with coefficients defined by the expressions (17), (18) with $r = a, b$, where hysteresis Preisach operator $P_S(t)$ appears in the denominator of nonlinear terms. In particular, setting $\omega_R = 0$, we arrive at a two two-patch modification of model (13) – (15) where the prey occupies both the neutral patch (which now plays the role of the risky patch) and the refuge under dangerous conditions and vacates the refuge, or its part, when the abundance of predator is low. A further extension of the model can be obtained by assuming that the volumes $\omega_R, \omega_S, \omega_0$ are functions of $\mathbf{x}$. This leads to a system with several Preisach operators, which have the same state at any given moment in time, but different weighting functions $\mu_i(\alpha_R, \alpha_S)$.

However, our assumption that the prey avoids some patches completely applies to all these models. This assumption is quite specific, because generally prey tends to occupy all the available space. Next, we replace complete avoidance by a more general assumption of an exchange flow with variable rate between the patches.

2.3. **Refuge analogy: flow between the patches.** We assume that the refuge consists of equal size small cells, which are embedded into a large free patch reservoir. The population rates are a_R, b_R, c_R in the free patch and a_S, b_S, c_S in the refuge cells. There is a fast flow of prey from each refuge cell to the free patch reservoir and backwards, a fast diffusion mixing in the free patch according to Assumption 6, but (for simplicity) no flow from cell to cell. Also, a fast diffusion process keeps the density of predator homogeneous in the whole habitat including the free patch and refuge cells. Let $\rho_S(\mathbf{x})$ be the density of prey in a refuge cell $\mathbf{x}$ and ρ_R be the density of prey in the free patch. Let $k_+(\mathbf{x})\rho_R$ be the prey flow rate from the free patch to a refuge cell $\mathbf{x}$ and $k_-(\mathbf{x})\rho_S(\mathbf{x})$ be the prey flow rate from the cell $\mathbf{x}$ to the free patch. That is, we assume proportionality of the rates to the prey density. Diffusion and exchange flows are assumed to have much faster time scale than population processes, hence ensuring the quasi-equilibrium relationship $k_-(\mathbf{x})\rho_S(\mathbf{x}) = k_+(\mathbf{x})\rho_R$ between the density of prey in the refuge cell $\mathbf{x}$ and the free patch. We apply an analog of Assumption 4 of the form

$$k_+(\mathbf{x})/k_-(\mathbf{x}) = f_R + (f_S - f_R)R_{\alpha_R(\mathbf{x}),\alpha_S(\mathbf{x})}[\eta(t_0)]A$$

with parameters $f_S > f_R \geq 0$ characterizing the ratio of the flow rates in and out of the refuge for two modes of prey's behaviour. For example, assuming the homogeneous constant flow rate $k_-(\mathbf{x}) = k_-$ from the refuge for all the cells $\mathbf{x}$, we postulate a higher rate $k_+(\mathbf{x}) = f_S k_-$ of the flow to the refuge when the prey switches to the safe mode of behaviour due to a high number of predator and a lower rate $k_+(\mathbf{x}) = f_R k_-$ of this flow when the number of predator drops and the prey returns to the risky behaviour. Again, the positive feedback mechanism

creates a separation of the switching thresholds $\alpha_R(\mathbf{x}) < \alpha_S(\mathbf{x})$, thus making the frightened prey stick to the refuge for lower values of the stimuli than those pushing the prey into the refuge.

Averaging the population rates over the refuge cells $\mathbf{x}$, we obtain the relations

$$\bar{r} = \frac{r_R\Omega_R + r_S\Omega_S f_R + r_S\Omega_S(f_S - f_R)P_S(t)}{\Omega_R + \Omega_S f_R + \Omega_S(f_S - f_R)P_S(t)}$$

for the average attack and birth rates $r = a, b$ and the formula

$$\bar{c} = \frac{c_R\Omega_R + c_S\Omega_S f_R^2 + c_S\Omega_S(f_S^2 - f_R^2)P_S(t)}{(\Omega_R + \Omega_S f_R + \Omega_S(f_S - f_R)P_S(t))^2}$$

for the average competition rate, where Ω_R is the volume of the free patch and Ω_S is the total volume of all the refuge cells. We see that these expressions have the same form as, and can be considered as a specific case of, the population rates (17), (18) in the model with repelling patches from the previous subsection. A similar model results from the assumption that the the exchange rate ratios f_R, f_S depend on $\mathbf{x}$.

In what follows, we perform a steady state analysis for the simplest representative from the class of models presented above, the system (13) – (15).

3. Steady state analysis

3.1. **Initial data.** In this section, we consider system (13) – (15), where the Preisach operator has the simple uniform density function (16). The rates are assumed to satisfy the relationships $b_S = b_R = b, c_S > c_R, a_S < a_R$, that is the birth rate is the same for both modes of prey's behaviour. Initial data for this system include initial values of the four variables: the number of prey u, the number of predator v, the proportion of prey in the safe mode of behaviour P_S, and the variable y measuring the value of stimuli as perceived by the prey; as well as the initial binary state function $\eta_0(\alpha_R, \alpha_S)$ of the Preisach operator, which defines the initial state (0 or 1) of each relay (2) in the integral formula (12) for P_S. At the initial moment t_0, the prey is in the safe mode of behaviour in all those cells that have switching thresholds α_R, α_S for which $\eta_0(\alpha_R, \alpha_S) = 1$; the cells containing prey in the risky mode have switching thresholds satisfying $\eta_0(\alpha_R, \alpha_S) = 0$. The initial data should satisfy two compatibility conditions. The first of them results from the fact that the state of a relay R_{α_R,α_S} is 0 whenever its input satisfies $A(t) \le \alpha_R$ and is 1 whenever $A(t) \ge \alpha_S$, see (2). Applying this rule at the initial moment to all the relays with the input $y(t_0)$, we obtain the condition

$$\eta_0(\alpha_R, \alpha_S) = \begin{cases} 0, & \alpha_R \ge y(t_0), \\ 1, & \alpha_S \le y(t_0). \end{cases} \tag{20}$$

CRM Preprint Series number 1215

For those pairs (α_R, α_S) that satisfy[2] $0 \le \alpha_R < y(t_0) < \alpha_S \le 1$ the value $\eta_0(\alpha_R, \alpha_S)$ can be either 0 or 1. The second compatibility condition arises from equation (15), which, using relations (12), (16), can be written at the initial moment as

$$P_S(t_0) = \int_0^1 \int_0^{\alpha_S} \eta_0(\alpha_R, \alpha_S)\, d\alpha_R d\alpha_S. \tag{21}$$

Combining (20) and (21), we see that initial data must satisfy the inequalities

$$\begin{array}{cc} P_S(t_0) = 0 & \text{if} \quad y(t_0) = 0, \\ y^2(t_0) \le P_S(t_0) \le y(t_0)(2 - y(t_0)) & \text{if} \quad 0 < y(t_0) < 1, \\ P_S(t_0) = 1 & \text{if} \quad y(t_0) \ge 1. \end{array} \tag{22}$$

In particular, if $y(t_0) = 0$ then $\eta_0(\alpha_R, \alpha_S)$ must identically equal zero (all prey in the risky mode of behaviour), whereas if $y(t_0) \ge 1$ then $\eta_0(\alpha_R, \alpha_S)$ must identically equal 1 (all prey in the safe mode). If strict inequalities hold in (22), that is $y^2(t_0) < P_S(t_0) < y(t_0)(2 - y(t_0))$ with $0 < y(t_0) < 1$, then there are infinitely many initial state functions $\eta_0(\alpha_R, \alpha_S)$ that satisfy compatibility conditions (20), (21).

3.2. **Equilibria of the system.** At an equilibrium, all the variables u, v, P_S, y are constant, and so is the state $R_{\alpha_R,\alpha_S}[\eta_0(\alpha_R, \alpha_S)]y = \eta_0(\alpha_R, \alpha_S)$ of each relay in (12). Therefore, equilibrium values of the four variables u, v, P_S, y satisfy three algebraic equations obtained by setting the right hand sides of differential equations (13) – (14) to zero; the operator equation (15) at an equilibrium is equivalent to (20) and thus results in the additional constraint (22), where $P_S(t_0)$ and $y(t_0)$ are now equilibrium values of the variables P_S and y.

A few remarks are in order before we calculate equilibria of system (13) – (15).

First, the constraint (22) has the form of a two-sided inequality if $0 < y < 1$. Hence, the four components of an equilibrium (u, v, P_S, y) with $0 < y < 1$ solve a system of three equations and two inequalities. Therefore, we expect such equilibria to form a continuous branch (or several branches), if they exist. Branches of equilibria are typical of systems with hysteresis due to the presence of the infinite dimensional component (space) of states η_0 of the hysteresis nonlinearity. Equilibria of system (13) – (15) with either $y = 0$ or $y > 1$ are isolated.

Secondly, equilibria embedded in a continuous branch can be neutrally stable, but not asymptotically stable.

Analysis of stability of equilibria is not a trivial problem. The reason is that the effect of a perturbation of the initial state function $\eta_0(\alpha_R, \alpha_S)$, which is part of the initial data, on the long term behaviour of a trajectory cannot be accounted for by a straightforward linearization approach. As an illustration, a robust equilibrium of a system with the Preisach operator can simultaneously attract many

[2] As $\mu(\alpha_R, \alpha_S) = 0$ outside the triangle $0 \le \alpha_R < \alpha_S \le 1$, we can restict the location of admissible pairs (α_R, α_S) to this triangle only.

CRM Preprint Series number 1215

trajectories and repel many trajectories from its neighborhood – a property which does not have an analog in the theory of smooth dynamical systems. For rigorous definitions and results (for planar differential systems coupled with the Preisach operator) we refer to [23], where such robust equilibria were called *partially stable*. Numerical results in [17, 24, 25] give an evidence that a continuous branch can include equilibria of different types, such as neutrally stable, partially stable, and unstable.

For some classes of differential equations with the Preisach operator, algorithms of rigorous local stability analysis based on linear approximations and conditions ensuring their validity were proposed [26, 27, 28, 29]. In this paper, we do not perform such analysis for system (13) – (15). Instead, we will resort to a number of numerical simulations in order to reveal some biologically relevant global scenarios of convergence of trajectories to, and divergence from, equilibrium points and branches.

Let us proceed with the calculation of equilibrium solutions. There is a unique equilibrium with zero prey population u. This is the trivial equilibrium $u = v = P_S = 0$ (where $v = 0$ follows from Eq. (14) and $P_S = 0$ follows from the first equation in (22)). The trivial equilibrium is unstable, because in its neighborhood the linear term bu with $b > 0$ dominates quadratic terms in Eq. (13); hence, for any small positive u and v, the u population exponentially increases.

There is another predator free equilibrium. With $v = 0$ Eqs. (22) imply $P_S = 0$ (all the prey in the risky mode) and from Eq. (13) we obtain a unique non-zero prey population $u = b/c_R$. In what follows, we assume that

$$ba_R e > c_R d. \tag{23}$$

Then, in a small neighborhood of the equilibrium $(u, v, P_S, y) = (b/c_R, 0, 0, 0)$, the right hand side of Eq. (14) is dominated by the linear term $(-d+ea_Rb/c_R)v$, which is positive for $v > 0$. Hence, the predator population exponentially increases, that is this equilibrium is also unstable.

All the other equilibrium points have all four positive components. Equations (13) – (14) for the positive equilibria imply

$$u = \frac{d}{e(a_S P_S + a_R(1 - P_S))}, \tag{24}$$

$$b = \frac{d(c_S P_S + c_R(1 - P_S))}{e(a_S P_S + a_R(1 - P_S))} + \frac{1}{\kappa}(a_S P_S + a_R(1 - P_S))y, \tag{25}$$

where $y = \kappa v$ due to (15), and Eq. (25) can be rewritten as

$$y = \frac{\gamma(1 - \theta P_S) - \mu(P_S + \gamma(1 - P_S))}{\nu(1 - \theta P_S)^2} =: F(P_S), \tag{26}$$

CRM Preprint Series number 1215

where we introduce new parameters

$$(27)\quad \gamma = \frac{c_R}{c_S} \in (0,1);\quad \theta = 1 - \frac{a_S}{a_R} \in (0,1);\quad \mu = \frac{c_R d}{a_R b e} \in (0,1);\quad \nu = \frac{a_R c_R}{b c_S \kappa} > 0;$$

the relation $\mu < 1$ is equivalent to (23). The function $y = F(P_S)$ defined by Eq. (26) satisfies

$$F(P_S) \to +0 \quad \text{as} \quad P_S \to -\infty; \qquad F(P_S) \to -\infty \quad \text{as} \quad P_S \to 1/\theta > 1$$

and has a unique point of local and global maximum on the interval $P_S < 1/\theta$; the graph Γ of F is shown in Fig. 2. For equilibria with $0 < y < 1$ (that is, equilibria with a non-zero fraction of prey in each of the two modes of behaviour), the additional constraint (22) defines the *lense* shaped domain $y^2 < P_S < y(2-y)$ between two parabolas, which lies inside the square $0 \le P_S, y \le 1$ of the (P_S, y) plane (see the same figure). Hence, any part Γ_i of the curve Γ contained in this lense domain defines a continuous curve of equilibria (u, v, P_S, y), $(P_S, y) \in \Gamma_i$ of system (13) – (15) with the components u, v related to the components P_S, y by Eqs. (24). In particular, if

$$(28)\qquad \gamma(1-\theta) < \mu + \nu(1-\theta)^2,$$

then $F(1) < 1$ and, due to $F(0) = \gamma(1-\mu)/\nu > 0$, the curve Γ intersects the lense domain, hence system (13) – (15) has at least one continuous branch of equilibrium points. The number of disjoint branches can vary from one to three depending on parameters as we discuss in the next subsection.

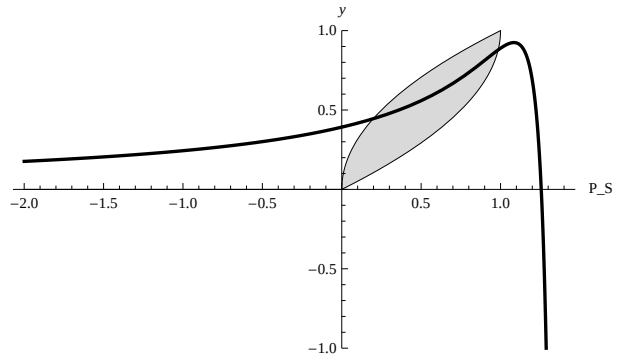

FIGURE 2. The intersection of the graph Γ of function (26) with the shaded lense domain is the projection of the curve of equilibrium points onto the (P_S, y) plane.

Eq. (28) ensures that all the positive equilibria satisfy $y < 1$, $P_S < 1$. That is, each positive equilibrium has a non-zero fraction of prey in the risky mode of behavior, as well as in the safe mode, and, generically, every positive equilibrium is embedded into a continuous branch of such equilibria. Additional parameter constraints can ensure that every trajectory enters the domain $P_S < 1$ and

CRM Preprint Series number 1215

remains there forever. One example is the relation

$$\mu + \theta > 1 \tag{29}$$

(which implies (28)). Indeed, Eq. (29) ensures that $\dot{v} = (-d + ea_S u)v < 0$ in Eq. (14) whenever $P_S = 1$, $v > 0$ and $u \le b/c_R$, while all trajectories enter the domain $u \le b/c_R$ and stay there forever, because Eq. (13) implies $\dot{u} \le (b - c_R u)$.

If the inequality $\gamma(1-\theta) > \mu + \nu(1-\theta)^2$, which is opposite to (28), holds, then system (13) – (15) has an isolated positive equilibrium with the components

$$u = d/(a_S e), \quad v = y/\kappa, \quad P_S = 1, \quad y = \frac{\gamma(1-\theta) - \mu}{\nu(1-\theta)^2}. \tag{30}$$

At this equilibrium, and in its neighborhood, all the prey is in the safe mode of behavior. Therefore, locally, system is equivalent to the ordinary differential predator-prey model (19), hence equilibrium (30) is asymptotically stable. It possibly coexists with a continuous branch of positive equilibria considered above, where prey have fractions of the population in both modes.

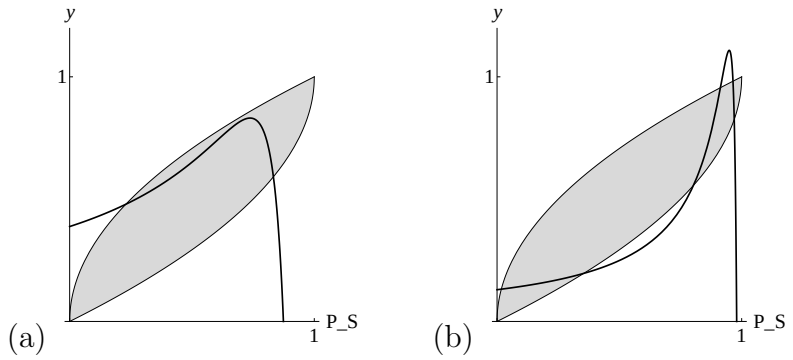

FIGURE 3. Different number of equilibrium branches of system (13) – (15). Panels show the projection of the branches on the (P_S, y) plane. (a) One branch for $\theta = 0.99$, $\gamma = 0.2$, $\mu = 0.03$, $\nu = 0.5$. The parameters satisfy condition (29). (b) Three branches for $\gamma = 0.065$, $\mu = 0.002$ with θ, ν same as for panel (a).

3.3. **Examples of branches of equilibria.** If $a_S \approx a_S$ and $c_R \approx c_S$ (equivalently, $\theta \ll 1, \gamma \approx 1$), then all the equilibria of system (13) – (15) are close to each other. This is to be expected as the change in attack and competion rates is small when prey switches between the safe and risky modes of behavior. If the attack rates are close to each other ($\theta \ll 1$), but the ratio γ of the competition rates is not close to one, then condition (28) ensures that the lense domain in Fig. 2 intersects the descending branch of the graph Γ of function (26). Hence, positive equilibrium points of the system form one continuous branch. On this branch, the equilibria with higher proportion P_S of prey in the safe mode of behavior have lower predator population. At the same time, Eq. (24) implies that

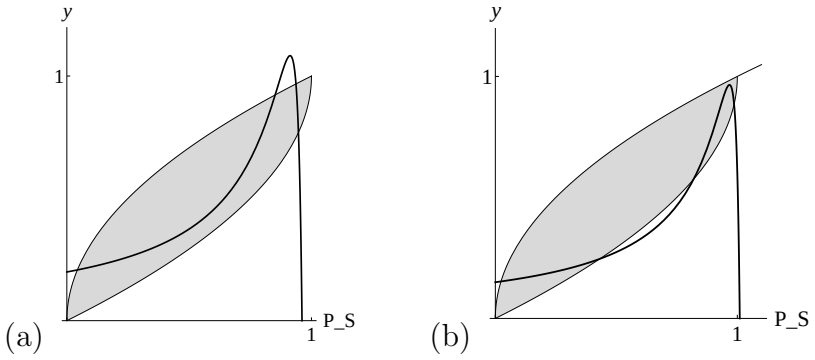

FIGURE 4. Examples with two branches of positive equilibrium points. (a) $\theta = 0.99$, $\gamma = 0.1$, $\mu = 0.005$. (b) $\theta = 0.95$, $\gamma = 0.075$, $\mu = 0.03$. The value of $\nu = 0.5$ is the same as for Fig. 3.

the number of prey u for all equilibrium points of the branch is almost the same due to $\theta \ll 1$.

The equilibrium branches become more interesting when the attack rates a_S and a_R are significantly different. If the ratio $a_S/a_R = 1-\theta$ is not too small, then, typically, the continuous branch of positive equilibria is still unique (assuming (28)). However, along this branch, the predator population v can either increase with P_S (the number of predator is higher for equilibria with higher fraction of safe prey), or decrease with increasing P_S (the number of predator is lower for equilibria with larger P_S), or v can achieve its maximum at an equilibrium with an intermediate value of P_S as in Fig. 3(a); we note that, according to Eq. (24), the number of prey u at an equilibrium always increases with P_S. The variations of the branch profile can be explained by looking at the unique positive equilibrium of the standard predator-prey system (19). The equilibrium predator population v of (19) tends to zero when the attack rate $\bar{a}$ either gets low or sufficiently high (in the latter case, the predator extincts after it eliminates the prey), hence v reaches its maximum bewteen these two extremes. Since in system (13) – (15) equilibria with different average attack rates $\bar{a} = a_R(1 - P_S) + a_S P_S$ coexist, increasing, decreasing and hump profiles of v with increasing P_S and u are all possible. A particular profile is defined by the relative position of the maximum of the curve Γ with respect to the lense domain, which determines the range of admissible average attack rates $\bar{a}$.

In the extreme of very different attack rates in the safe and risky modes of prey's behavior, $\theta \approx 1$, system (13) – (15) can have up to three disjoint continuous branches of equilibrium points. Fig. 3(b) presents an example where the curve Γ has three disjoint intersections with the lense domain, representing three equilibrium branches; Fig. 4 shows examples with two branches. In these figures, the value of the attack rate a_S is 1-5% of the value of the attack rate a_R. Also,

CRM Preprint Series number 1215

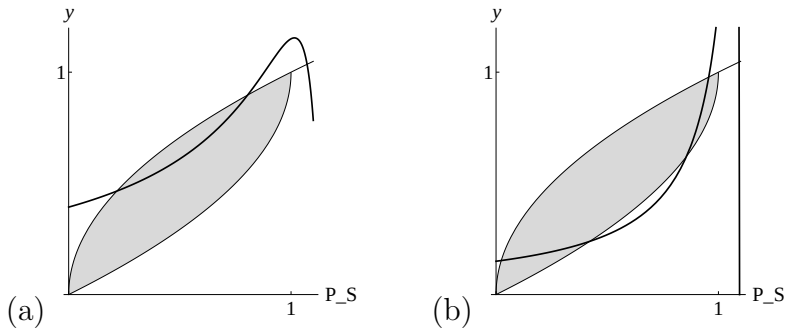

FIGURE 5. Examples with two (panel (a)) and three (panel (b)) branches of positive equilibrium points where the upper branch consists of one equilibrium with $P_S = 1$. (a) $\theta = 0.8$, $\gamma = 0.2$, $\mu = 0.017$. (b) $\theta = 0.95$, $\gamma = 0.075$, $\mu = 0.001$. The value of $\nu = 0.5$ is the same as for Fig. 3.

μ is small (for example, due to the small ratio of the death rate of the predator and birth rate of the prey, $d/b \ll 1$).

Parameters in Figs. 3, 4 satisfy the condition (28). Geometrically it means that the curve Γ passes below the upper corner $(1, 1)$ of the lense domain. We have seen that in this case all the equilibrium solutions have a non-zero fraction of prey in the risky mode, $P_S < 1$, wheras if $\gamma(1-\theta) > \mu + \nu(1-\theta)^2$ (that is, the curve Γ passes above the right corner of the lense), then the system has an isolated positive stable equilibrium where all the prey is in the safe mode, $P_S = 1$. In particular, this isolated saturated equilibrium is unique when Γ does not intersect the lense domain. Fig. 5 shows examples where the isolated equilibrium with $P_S = 1$ coexists with either one or two branches of equilibrium points with $P_S < 1$.

3.4. **Global dynamics: numerical results.** In this section, we present some results of numerical solution of Eqs. (13) – (15). We fix a parameter set such that the system has three disjoint continuous branches of equilibria as in Fig. 3(b) and attempt to charecterise stability of the steady states belonging to each of these branches. Initial values $u(t_0), v(t_0), P_S(t_0)$ and the initial state $\eta_0(\alpha_R, \alpha_S)$ of the Preisach model at the moment $t_0 = 0$ determine which equilibrium the solution converges to (see Fig. 7). In order to satisfy the compatibility conditions for the initial data, we introduce an auxiliary parameter $\xi \in [0, 1]$ and define the initial value $P_S(t_0)$ using the relationship $P_S(t_0) = P_S(t_0, \xi)$, where

$$P_S(\cdot, \xi) = (2\xi - 1)y^2(\cdot) + 2(1-\xi)y(\cdot), \tag{31}$$

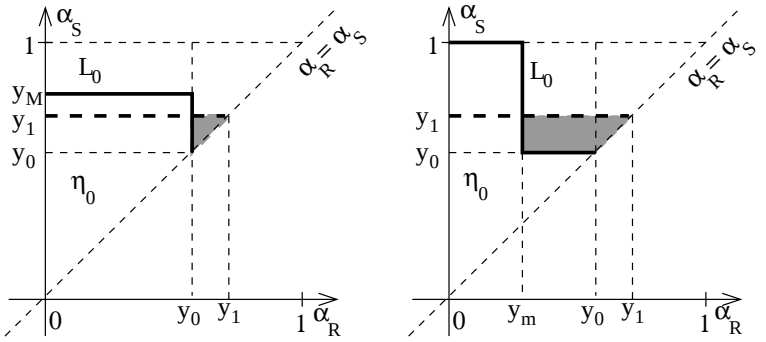

FIGURE 6. Configuration of initial data $\eta_0(\alpha_R, \alpha_S)$ such that the line L_0 has a vertical segment starting from $\alpha_R = \alpha_S = y_0$ (left) and a horizontal segment (right), bold solid lines. Change of configuration of the state, when the input increases from y_0 to y_1, is represented by bold dashed lines, and the gray areas show the relays R_{α_R,α_S} that were switched on after the increase of the input.

which ensures the compatibility condition (22) for an arbitrary choice of $y(t_0) = \kappa v(t_0)$. Furthermore, we use the following standard class of the so-called "staircase" states $\eta_0(\alpha_R, \alpha_S)$ of the Preisach operator, see [21, 22, 30], which are convenient to depict on the plane (α_R, α_S) (see Fig. 6). A state is defined by a continuous staircase line L_0 such that for all points (α_R, α_S) located to the left of (below) the line L_0 in the triangle $0 \le \alpha_R \le \alpha_S \le 1$ the relation $\eta_0(\alpha_R, \alpha_S) = 1$ is satisfied, while for all the other points of this triangle $\eta_0(\alpha_R, \alpha_S) = 0$. The polyline L_0 consists of horizontal and vertical segments (links), goes from North-West to South-East, and intersects the bisector $\alpha_R = \alpha_S$ at the point $(y(t_0), y(t_0))$. These properties ensure the compatibility condition (20). We note that for any given set of initial data $u(t_0), v(t_0), y(t_0)$ and $\xi \in (0, 1)$ with $P_S(t_0)$ defined by (31) there are still infinitely many choices of the staircase initial state satisfying the compatibility condition (21). For numerical simulations, we used initial states where the line L_0 has two links. Namely, there are two types of such states. For the first type, which we call V-type, the line L_0 consists of a segment of the vertical line $\alpha_R = y(t_0)$ and a segment of a horizontal line $\alpha_S = y_M > y(t_0)$ (see Fig. 6(a)). For the second type, called H-type, L_0 consists of a segment of the horizontal line $\alpha_S = y(t_0)$ and a segment of a vertical line $\alpha_R = y_m < y(t_0)$ (see Fig. 6(b)). The compatibility condition (21) implies the formula $y_M = y_M(\xi, y(t_0))$ for the corner point $(y(t_0), y_M)$ of the L_0-line of the V-type initial state and the relation $y_m = y_m(\xi, y(t_0))$ for the corner point $(y_m, y(t_0))$ of the H-type initial state, where

$$y_M(\xi, y_0) = ((1+\xi)y_0 + (1-\xi)(2-y_0))/2, \qquad y_m(\xi, y_0) = (1-\xi)y_0. \tag{32}$$

After the initial moment $t_0 = 0$, the staircase polyline L_0 changes in response to the variations of the input $y(t)$ to the Preisach operator according to a set of rules which can be found in [21, 30, 22, 31]; we do not discuss them here.

We perform numerical stability analysis of three disjoint continuous branches of equilibria of system (13) – (15) (as in Fig. 3(b)) by choosing appropriate parameters and perturbing initial state of the system in different ways (see Table 3.4). To illustrate these results, some of the obtained time traces of the predator population are presented in Fig. 7. The initial conditions $u(0), v(0), P_S(0)$, and η_0 for each solution were selected from a close vicinity of a steady state by taking the following steps. First, we fixed a value of $\xi \in [0, 1]$ and solved equations (24), (25), (31) to obtain three equilibrium points (u^*, v^*, P_S^*), one on each of the three branches. Next, we slightly perturbed the predator number from its equilibrium value v^* and used the initial data $v(0) = v^* + \delta v$, $u(0) = u^*$, $P_S(0) = P_S^*$ to perform a simulation. The initial state η_0 of the Preisach operator was either of V-type or H-type for each simulation.

The branches of equilibria can be uniquely identified by the proportion of prey in the safe mode P_S as the ranges of P_S for the three branches are disjoint, see Fig. 3(b); we denote the left branch by (L), the middle branch by (M) and the right branch by (R). An equilibrium on a particular branch is identified by the value of $\xi \in [0, 1]$. We have used $\xi = 0.7$ to obtain results listed in Table 3.4 and plotted on Fig. 7. The corresponding values of v^*, P_S^* at the equilibrium are $v^* = 0.99731586, P_S^* = 0.99624508$ for branch (R), $v^* = 0.892, P_S^* = 0.8535$ for branch (M), and $v^* = 0.1593, P_S^* = 0.1065$ for branch (L). That is, the predator is most abundant at the equilibrium on branch (R) and least abundant on branch (L). We have also performed simulations with different values of ξ and different types of perturbations, where we have perturbed initial values of u, P_S and the initial state of the Preisach operator, and we have found that Fig. 7 represents well the dynamics we observed. In particular, our simulations show that the steady states on branch (R) (see Table 3.4(a)-(d), graphs (a), (d) in Fig. 7) and on branch (L) (see Table 3.4(i)-(l), Fig. 7(i)) are neutrally stable: the perturbed solution converges to an equilibrium belonging to the same branch with the value $\tilde{\xi}$ close to 0.7. The destination equilibrium where the trajectory converges to depends on the magnitude and sign of the perturbation. For example, the value $|\tilde{\xi} - 0.7|$ is much larger for trajectory (b) where $\delta v = 10^{-7}$ than for trajectory (a) where $\delta v = -0.001$ (see Table 3.4).

The most interesting behaviour was observed for perturbations of equilibrium points from branch (M). For the H-type initial state η_0 of the Preisach operator, we found that the trajectory diverges from this branch and converges to an equilibrium on branch (R) for positive small perturbations of initial predator abundance, see trajectory (e) in Table 3.4, Fig. 7. However, for negative perturbations the solution converges to an equilibrium on the same branch (M) as before (see Table 3.4(f)). Moreover, for the V-type initial state η_0, the solution converges

CRM Preprint Series number 1215

to a nearby equilibrium on branch (M) for arbitrary small perturbations, see Table 3.4(g)-(h), Fig. 7(g), (h). Thus, equilibrium points from the middle branch (M) demonstrate simultaneously repelling and attracting properties. Such equilibria have been characterised as *partially stable* in [23] (where equilibria were isolated rather than embedded in a branch though). The property to attract many trajectories and simultaneously repel many trajectories should be attributed to the memory properties of system (13) – (15). In the theory of ordinary differential systems, an analogous behaviour is demonstrated by a saddle-node equilibrium. However, a saddle-node is not robust to arbitrarily small perturbations, whereas the partially stable equilibrium branch (M) of system (13) – (15) is robust.

Solution	Branch	η_0 type	δv	v^{**}	P_S^{**}	$\tilde{\xi}$
(a)	R	H	10^{-7}	0.997188	0.99624521	0.6672
(b)	R	H	-0.001	0.997317	0.99624508	0.7003
(c)	R	V	10^{-7}	0.9972621	0.99624513	0.6862
(d)	R	V	-10^{-7}	0.997447239	0.99624495	0.736
(e)	M	H	0.001	0.9974308842	0.99624497	0.7314
(f)	M	H	-0.001	0.8911	0.8533	0.6943
(g)	M	V	0.001	0.8989	0.8548	0.7427
(h)	M	V	$0.001^{(*)}$	0.8864	0.8525	0.6686
(i)	L	H	0.001	0.1597	0.1065	0.6985
(j)	L	H	-0.001	0.159	0.1054	0.7004
(k)	L	V	0.001	0.1595	0.1056	0.701
(l)	L	V	-0.001	0.1589	0.105	0.7015

TABLE 1. Initial data and destination point for solutions obtained by different perturbations of three equilibrium points $v^* = 0.99731586, P_S^* = 0.99624508$ for branch (R), $v^* = 0.892, P_S^* = 0.8535$ for branch (M), and $v^* = 0.1593, P_S^* = 0.1065$ .The columns specify the solution; branch of equilibria near which the solution starts (a particular equilibrium near which the solution starts is defined by the parameter $\xi = 0.7$); type of initial state η_0; value of the perturbation δv for the initial value $v(0) = v^* + \delta v$ of the solution (other perturbations are $\delta u = \delta P_S = 0$, that is $u(0) = u^*$, $P_S = P_S^*$, except for solution (h) where also the initial state η_0 was perturbed); components v^{**}, P_S^{**} of the equilibrium to which the solution converges; the value $\tilde{\xi}$ of the parameter ξ for the equilibrium to which the solution converges.

CRM Preprint Series number 1215

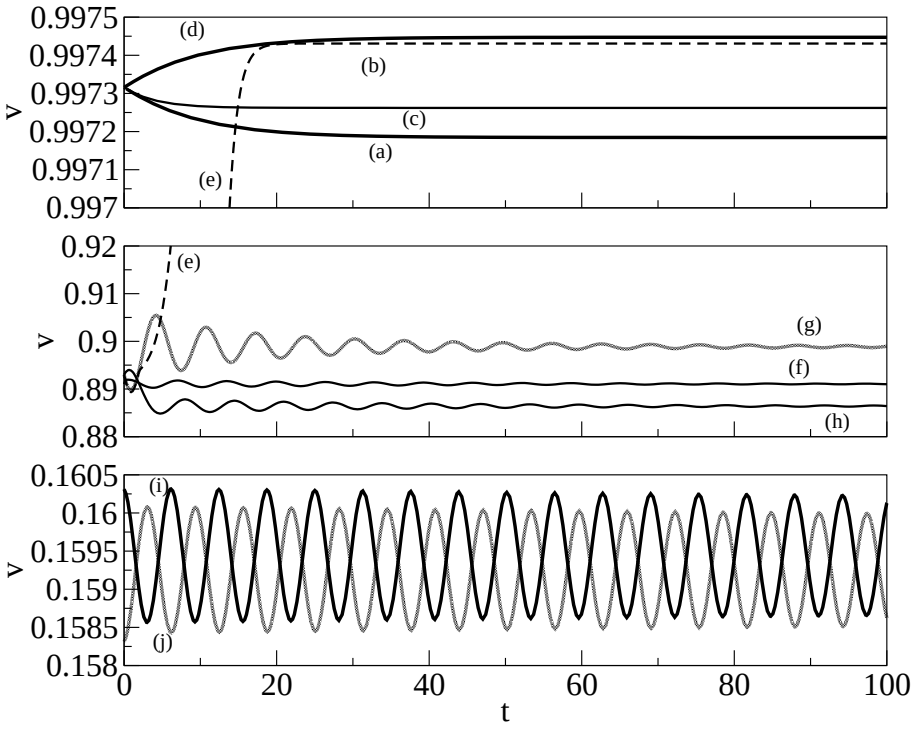

FIGURE 7. Time traces of the predator population v of system (13) – (15). Parameters are $b = d = \kappa = 1$, $\theta = 0.993$, $\nu = 1.4$, $\gamma = 0.2$, $\mu = 0.002$. Initial data for each solution are summarized in Table 3.4. The dashed solution (e) starts near the equilibrium branch (M) and converges to an equilibrium belonging to branch (R). Solution (i) converge slowly to an equilibrium and look like periodic oscillations for the values of t that are shown. This behaviour is explained by Figure 8(b): real part of one of the eigenvalues is close to 0 for $\xi \approx 0.7$ in the analogous ordinary differential system (13), (14), (31). **Trajectrory (e) deserves a line of discussion in the text.**

For comparison, let us consider an ordinary differential system (13), (14), (31), where the proportion of the prey population in the safe mode P_S is a (memoryless) function of the perceived stimuli $A = \kappa v$, which depends on an additional parameter $\xi \in [0, 1]$. The union of all the steady states (u^*, v^*, P_S^*) of this system for all $\xi \in [0, 1]$ coincides with the set of the steady states of system (13) – (15). Fig. 8(a) presents three branches of equilibrium points for the parameter set of Fig. 7. Here, system (13), (14), (31) has three equilibrium points for each ξ (cf. Fig. 3(b)). The linear stability analysis shows that the equilibrium points with the most abundant and the least abundant predator population (the upper and lower branches in Fig. 8(a) corresponding to the branches (R) and (L), respectively, on Fig. 3(b)) are asymptotically stable, whereas the the equilibrium

at the middle branch is a saddle. Fig. 8(b) presents the maximal real part of the eigenvalues of the linearization at each equilibrium of system (13), (14), (31).

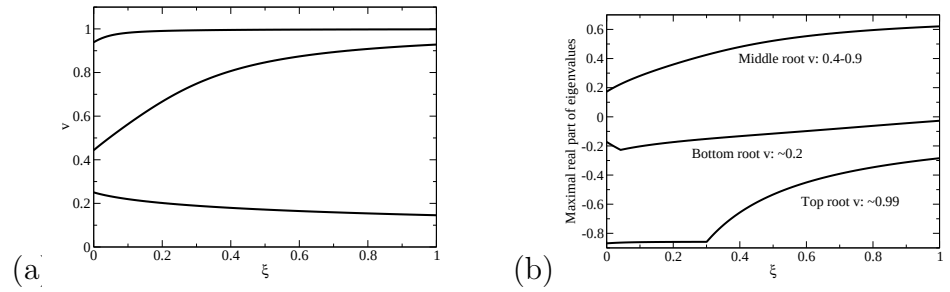

FIGURE 8. Bifurcation diagrams for ordinary differential system (13), (14), (31). (a) The dependence of equilibrium predator population on the parameter ξ for three branches of positive equilibria. (b) Maximal real part of the eigenvalues of the linearization at equilibrium points. Parameters are the same as in Fig. 7.

We see that ordinary differential system (13), (14), (31) demonstrates a typical predator pit scenario, which is characterized by two stable and one unstable equilibria. In model (13) – (15), in comparison, isolated locally stable equilibria are replaced by continuous branches of neutrally stable equilibria. The branch of equilibrium points, which corresponds to the unstable equilibrium of the ordinary differential model, is partially stable: equilibria of this branch are neutrally stable for V-type initial memory state of the Preisach operator, and unstable for the H-type initial state.

4. Conclusions

The predator-prey relationship, where one class of animal — the predator — kills and consumes animals of another group — the prey, is of fundamental importance in ecology. Both groups of this system, however, are subject to similar evolutionary demands i.e. they seek to maximise individual fitness. Therefore, both the predator and the prey strive to maximise their own individual survival and reproductive success. Much is known about the adaptations of predators in the detection, pursuit and subduing of prey (e.g., [32]) and the evolutionary responses of their quarry, including aposomatic colouration and crypsis (e.g., [33]), autotomy, group living and selfish herd behaviour [34] , and the use of the looming image (e.g., [35]). Indeed the whole predator - prey interaction has been depicted as an "Arms Race" ([36], see also [37]).

Less is known however about the subtle behavioural responses of prey to the presence of predators. Prey live in a "landscape of fear" [38, 39, 40] and this ambiance of threat imposes costs (e.g., [41, 42, 43]) including the increased allocation of time to vigilance and to hiding, and the general "trade off in energy for

CRM Preprint Series number 1215

safety made by foraging animals" [42]. Indeed there is now much focus on the "non-lethal effects" of predators [44]. Predators can have a direct adverse impact on prey population density — the "consumptive effect" and/or by altering their behaviour, the "non-consumptive" effect [45].

The "fear" of being killed is a non-consumptive effect and it raises the issue of decision making and the taking of risks. The phenomenon of fear is highly complex (e.g., [46]; Kagen, 20013; [47, 48]). In mammals, and perhaps in birds, fear memory is located in the amygdala whereas spatial memories are stored in the hippocampus (e.g., [47]). However, animals have to feed themselves and provision their young, so in the landscape with predators they have to take risks.

It would appear that the acquisition of fear and the development of defensive responses through, for example, Pavlovian conditioning or associative learning is at least in part a hysteresis (see [45, 46, 49]). Presumably fear may have a lasting effect on animal's behavior even after the environment has become less dangerous. By this reason, the Preisach operator seems to provide us with a suitable tool for modeling this form of adaptive response as a permanent effect of temporary stimuli (PETS). In particular, the phenomenology of the Preisach model based on superposition of simple bi-stable responses of many individuals is attractive for modeling population processes.

The presence of hysteresis and hysteretic patterns of behaviour of individual species have been described for various ecological systems [50, 51, 52]. However, the most accurate measurements of multi-stability and hysteresis were obtained for microorganisms in laboratory experiments [53, 54, 55, 56, 57, 58, 59, 60, 61]. The importance of bi-stability in living systems has been first articulated by Max Delbrück [62], who associated different stationary states with epigenetic differences in clonal populations of microorganisms. A classical example of bi-stable behavior in bacteria is provided by lac-operon, a collection of genes which are associated with transport and metabolism of lactose in *E. coli*. Expression of these genes can be turned on by molecules called inducers. Novick and Weiner [63] as well as of Cohn and Horibata [64, 65, 66] demonstrated that two phenotypes each associated with "on" and "off" state of *lac-operon* expression can be obtained from the same culture of genetically identical bacteria. Novick and Weiner did not use the term "hysteresis", but effectively they described the response of the lac-operon to variation of the extracellular concentration of inducers as a bi-stable switch with two different switching thresholds, and their early findings of hysteresis were consistent with even earlier observations of bi-stability of enzymes in yeast [67]. Recent experiments using molecular biology methods permitted to confirm and further study the region of bi-stability of the *lac-operon* when multiple input variables are used to switch the *lac-operon* genes on and off. On the other hand, reaction diffusion differential equations where bacteria were modeled by bi-stable switches are capable of explaining experimentally observed pattern formation in bacterial colonies [Jaeger-Hoppenstedt].

CRM Preprint Series number 1215

The idea that adaptation to time-varying environments through switching of behavior of phenotype helps survival and that organisms use various switching strategies (such as bet-hedging, matching the switching rate to the rate of environmental changes, etc.) to increase their fitness has been discussed in different biological contexts and gained a substantial experimental support [68, 69, 70, 71, 72, 73]. The model proposed in [74] shows that a switching strategy based on a bi-stable hysteresis can be advantageous when a realistic opportunity cost is associated with any phenotype switching event. Bi-stability allows organisms avoid excessive switching when favoring of the more favored over the less favored phenotype is not strong and the loss incurred by the transition event exceeds the gain from being in the state favored by the environment. This observation (that agrees with some experimental findings [75, 76]) is rather general and can be extended to adaptative behavior in predator-prey interaction. One can therefore conjecture that hysteresis in adaptive response may develop as an optimal switching strategy. As we discussed in Section 2, hysteresis in decision making can also develop as a result of herding behavior when an individual tends to follow others. The simplest model demonstrating this effect consists of two identical coupled memoryless switches (step functions): indeed, this system responds to external inputs exactly as one bi-stable switch with two different thresholds [devilstaircase]. Effectively, hysteresis develops through a positive feedback loop resulting in the separation of switching thresholds and creation of a bi-stability range. Large systems of interacting memoryless switches, such as in the Ising model [networks, brain, sociology, sir], produce complex hysteresis loops, which are similar to those of the Preisach model [Sethna].

The results obtained in his work can be compared to the outcomes of the ordinary differential model proposed in [9], which has a similar structure except that the adaptive response in [9] is memoryless. The ordinary differential model demonstrated the co-existence of two stable positive equilibrium states with high and low prey population, which were separated by a separatrix of a saddle point. The introduction of memory in the adaptive response, which has been implemented in this paper, results in a "blow up" of each equilibrium into a connected continuum (branch) of equilibrium states. Some of these three branches may also merge so that the set of all equilibriums may have from one to three connected components depending on the parameter regime. Each equilibrium state within a given branch is characterised by a different proportion of the prey population that adopted the safe mode of behaviour. As a result, we observe that trajectories converge to a "continuous spectrum" of equilibrium states. Typically, trajectories starting from close initial conditions converge to close (but different) equilibrium states. Furthermore, this convergence can be characterised as path-dependent (a concept used in economics and social sciences). The trajectories along which the predator population achieves a higher peak tend to end up at an equilibrium with higher proportion of prey in the refuge (safe mode of behaviour) and a higher total population of prey. This can be explained by the effect of the memory.

CRM Preprint Series number 1215

Indeed, when the predator population peaks, the prey hides in the refuge, and even after the predator numbers subside a substantial part of the prey population (with low enough threshold α_R) remains in the refuge due to the memory of the outburst of predator's population that the prey experienced in the past.

Memory induced multiplicity of equilibrium states has been observed also in the SIR model developed in [17]. However, the cost of safety, which we introduce in the predator-prey model in this paper, produces further interesting behaviour. In the regime with three disjoint branches of equilibrium points, most trajectories converge either to the "upper branch" (where the prey population is high), or to the "lowest branch" (with a low prey population at each equilibrium). However, the "middle branch" does not quite behave as a separatrix between the basins of attraction of these two branches as one might expect using the intuition of smooth dynamical systems theory. Some small perturbations of initial data result in a trajectory that leads from an equilibrium state E on the middle branch either to the upper or to the lower branch, while other small perturbations of the same equilibrium E produce just a short trajectory that ends at a nearby equilibrium on the same middle branch. This behaviour has a similarity with a saddle-node point of smooth dynamical systems which simultaneously attracts and repels many trajectories. However a saddle node point is structurally unstable and can be eliminated by a small perturbation of parameters, while equilibrium states of our system are structurally stable (robust to parameter perturbations). We call such robust equilibrium states E partially stable. (Theoretical analysis of partially stable equilibria of systems with hysteresis has been done in part in [fixedpoint,homoclinic1,homoclinic2] and will be a subject of future study.) In a sense, hysteresis introduced into the adaptive response grants more stability to the middle equilibrium point.

The conceptual methodology, which we exploited in this paper, and in particularly the concept of a dependence of a model parameters on certain stimuli, which in their turn depend on the current and past state variables, and modelling memory by a hysteresis, are not limited to the considered Lotka-Volterra model (which was used here mostly as a convenient case study), but can be straightforwardly extended to any other model when adaptation or memory (or both) should be studied.

Acknowledgements. A. P. acknowledges the support of SFB 787 of the DFG, project B5. A. K. is supported by the Ministry of Science and Innovation of Spain via Ramón y Cajal Fellowship RYC-2011-08061 and grant MTM2011-29342, by CONACYT (Mexico) via grant N219614, and by AGAUR (Generalitat de Catalunya) via grant 2014SGR-1307. D. R. acknowledges the support of NSF through grant DMS-1413223.

References

[1] E. Kandel. The molecular biology of memory storage: A dialogue between genes and synapses. *Science*, 294:10301038, 2001.

[2] R. D. Hawkins, E. Kandel, and C. B. Bailey. Molecular mechanisms of memory storage in aplysia. *Biological Bulletin*, 210:174191, 2006.

[3] R. Menzel, U. Greggers, A. Smith, S. Berger, S. Brandt, G. Bundrock, T. Plumpe, F. Schaupp, S. Silke, J. Stindt, N. Stollhoff, and S. Watzl. Honey bees navigate according to a map-like memory. *Proceedings of the National Academy of Sciences*, 102:30403045, 2006.

[4] T. S. Collett and M. Collett. Memory use in insect visual navigation. *Nature Reviews Neuroscience*, 3:542552, 2002.

[5] N. S. Clayton, D. P. Griffiths, N. J. Emery, and A. Dickinson. Elements of episodic memory in animals. *Phil. Trans. R. Soc. Lond B*, 356:14831491, 2001.

[6] N. J. Emery and N. S. Clayton. Effects of experience and social context of prospective caching strategies in scrub jays. *Nature*, 414:443446, 2004.

[7] N. J. Emery, J. Dally, and N. S. Clayton. Western scrub jays (aphelocoma californica) use cognitive strategies to protect heir caches from thieving conspecifics. *Animal Cognition*, 7:3743, 2004.

[8] E. Tulving. Episodic memory: From mind to brain. *Ann. Rev. Psychology*, 53:125, 2002.

[9] A. Pimenov, T. C. Kelly, A. Korobeinikov, M. J. A. O'Callaghan, and D. Rachinskii. Adaptive behaviour and multiple equilibrium states in a predator-prey model. *Theoretical Population Biology*, 101:24–30, 2015.

[10] James M. McNair. The effects of refuges on predator-prey interactions: A reconsideration. *Theoretical Population Ecology*, 29:38–63, 1986.

[11] Alan R. Hausrath. Analysis of a model predator-prey system with refuges. *Journal of Mathematical Analysis and Applications*, 181:531–545, 1994.

[12] Vlastimil Krivan. Evolutionary games and population dynamics. In P. Drabek, editor, *Proceedings of Seminar in Differential Equations, Kamenice nad Lipou*, volume II, pages 223–233. Vydavatelsky servis, Plzen, 2009.

[13] Giovanna Chiorino, Pierre Auger, Jean-Luc Chassé, and Sandrine Charles. Behavioral choices based on patch selection: a model using aggregation methods. *Mathematical Biosciences*, 157:189–216, 1999.

[14] G. D. Ruxton. Short term refuge use and stability of predator-prey models. *Theoretical Population Ecology*, 47:1–17, 1995.

[15] Daniel T Blumstein and Janice C Daniel. The loss of anti-predator behaviour following isolation on islands. *Proceedings of the Royal Society of London B: Biological Sciences*, 272(1573):1663–1668, 2005.

[16] Guy Beauchamp. Reduced flocking by birds on islands with relaxed predation. *Proceedings of the Royal Society of London, Series B: Biological Sciences*, 271(1543):1039–1042, 2004.

[17] Alexander Pimenov, Tom C. Kelly, Andrei Korobeinikov, Michael J.A. O'Callaghan, Alexei V. Pokrovskii, and Dmitrii Rachinskii. Memory effects in population dynamics: Spread of infectious disease as a case study. *Mathematical Modelling of Natural Phenomena*, 7:204–226, 2012.

[18] Alexander Pimenov, Tom C. Kelly, Andrei Korobeinikov, Michael J.A. O'Callaghan, and Alexei V. Pokrovskii. Systems with hysteresis in mathematical biology via a canonical example. In Caroline L. Wilson, editor, *Mathematical Modeling, Clustering Algorithms and Applications*, page 10. Nova Science Publishers, 2010.

[19] Evan L. Preisser, Daniel I. Bolnick, and Michael F. Benard. Scared to death? the effects of intimidation and consumption in predatorprey interactions. *Ecology*, 86:501–509, 2005.

CRM Preprint Series number 1215

[20] Evan L. Preisser and Daniel I. Bolnick. The many faces of fear: Comparing the pathways and impacts of nonconsumptive predator effects on prey populations. *PLoS ONE*, 3:e2465, 2008.

[21] M. A. Krasnosel'skii and A. V. Pokrovskii. *Systems with Hysteresis*. Springer, New York, 1989. Zbl 0665.47038, MR0987431.

[22] I. Mayergoyz. *Mathematical Models of Hysteresis and Their Applications*. Elsevier, 2003. Zbl 0723.73003, MR1083150.

[23] S. McCarthy and D. Rachinskii. Dynamics of systems with Preisach memory near equilibria. *Mathematica Bohemica*, 139:39–73, 2014.

[24] A. Pimenov and D. Rachinskii. Homoclinic orbits in a two-patch predator-prey model with preisach hysteresis operator. *Mathematica Bohemica*, 139(2):285–298, 2014.

[25] A. Pimenov and D. Rachinskii. Robust homoclinic orbits in planar systems with preisach hysteresis operator. *WIAS Preprint*, 1994:1, 2014.

[26] A. Pimenov and D. Rachinskii. Linear stability analysis of systems with Preisach memory. *Discrete and Continuous Dynamical Systems - Series B*, 11(4):997–1018, 2009. Zbl 1181.47075, MR2505656, DOI 10.3934/dcdsb.2009.11.997.

[27] A. Pokrovskii, T. Power, D. Rachinskii, and A. Zhezherun. Differentiability of evolution operators for dynamical systems with hysteresis. *Journal of Physics: Conference Series*, 55:171, 2006. DOI 10.1088/1742-6596/55/1/017.

[28] P. Krejčí, J. P. O'Kane, A. Pokrovskii, and D. Rachinskii. Stability results for a soil model with singular hysteretic hydrology. *Journal of Physics: Conference Series*, 268(1):012016, 2011. DOI 10.1088/1742-6596/268/1/012016.

[29] M. Brokate, A.V. Pokrovskii, D.I. Rachinskii, and O. Rasskazov. Differential equations with hysteresis via a canonical example. In Isaak Mayergoyz and Giorgio Bertotti, editors, *The Science of Hysteresis*, volume I, chapter II, pages 125–291. Elsevier, Academic Press, 2005. Zbl 1142.34026, MR2307929.

[30] M. Brokate and J. Sprekels. *Hysteresis and Phase Transitions*. Springer, Berlin, 1996. Zbl 0951.74002, MR1411908.

[31] P. Krejčí. *Hysteresis, Convexity and Dissipation in Hyperbolic Equations*. Gakkotosho, Tokyo, 1996. Zbl 1187.35003, MR2466538.

[32] M. Begon, C. R. Townsend, and J. L. Harper. *Ecology: From Individuals to Ecosystems*. Wiley-Blackwell, 2006.

[33] Nicholas B Davies, John R Krebs, and Stuart A West. *An introduction to behavioural ecology*. John Wiley & Sons, 2012.

[34] William D Hamilton. Geometry for the selfish herd. *Journal of theoretical Biology*, 31(2):295–311, 1971.

[35] Steven L Lima and Lawrence M Dill. Behavioral decisions made under the risk of predation: a review and prospectus. *Canadian Journal of Zoology*, 68(4):619–640, 1990.

[36] Richard Dawkins and John R Krebs. Arms races between and within species. *Proceedings of the Royal Society of London B: Biological Sciences*, 205(1161):489–511, 1979.

[37] Edmund D. Brodie and Edmund D. Brodie. Predator-prey arms races: Asymmetrical selection on predators and prey may be reduced when prey are dangerous. *BioScience*, 49(7):557–568, 1999.

[38] Kelly B Altendorf, John W Laundré, Carlos A López González, and Joel S Brown. Assessing effects of predation risk on foraging behavior of mule deer. *Journal of Mammalogy*, 82(2):430–439, 2001.

[39] John W Laundré, Lucina Hernández, and Kelly B Altendorf. Wolves, elk, and bison: reestablishing the" landscape of fear" in yellowstone national park, usa. *Canadian Journal of Zoology*, 79(8):1401–1409, 2001.

CRM Preprint Series number 1215

[40] John W Laundré, Lucina Hernández, and William J Ripple. The landscape of fear: ecological implications of being afraid. *Open Ecology Journal*, 3:1–7, 2010.
[41] Theodore Stankowich and Daniel T Blumstein. Fear in animals: a meta-analysis and review of risk assessment. *Proceedings of the Royal Society of London B: Biological Sciences*, 272(1581):2627–2634, 2005.
[42] Kate R Searle, Chris J Stokes, and Iain J Gordon. When foraging and fear meet: using foraging hierarchies to inform assessments of landscapes of fear. *Behavioral Ecology*, 19(3):475–482, 2008.
[43] Liana Y Zanette, Aija F White, Marek C Allen, and Michael Clinchy. Perceived predation risk reduces the number of offspring songbirds produce per year. *Science*, 334(6061):1398–1401, 2011.
[44] Will Cresswell. Non-lethal effects of predation in birds. *Ibis*, 150(1):3–17, 2008.
[45] Sara L Hermann and Jennifer S Thaler. Prey perception of predation risk: volatile chemical cues mediate non-consumptive effects of a predator on a herbivorous insect. *Oecologia*, 176(3):669–676, 2014.
[46] Joseph E LeDoux. Coming to terms with fear. *Proceedings of the National Academy of Sciences*, 111(8):2871–2878, 2014.
[47] Donna J Cross, John M Marzluff, Ila Palmquist, Satoshi Minoshima, Toru Shimizu, and Robert Miyaoka. Distinct neural circuits underlie assessment of a diversity of natural dangers by american crows. *Proceedings of the Royal Society of London B: Biological Sciences*, 280(1765):20131046, 2013.
[48] Philip Tovote, Jonathan Paul Fadok, and Andreas Lüthi. Neuronal circuits for fear and anxiety. *Nature Reviews Neuroscience*, 16(6):317–331, 2015.
[49] Sevil Duvarci and Denis Pare. Amygdala microcircuits controlling learned fear. *Neuron*, 82(5):966–980, 2014.
[50] John H. Costello, J. Rudi Strickler, Celia Marrasé, Geoff Trager, Robert Zeller, and Amy J. Freise. Grazing in a turbulent environment: Behavioural response of a calanoid copepod, contropages hamatus. *Proc. Natl. Acad. Sci. USA*, 87:1648–1652, 1990.
[51] Peter A. Jumars. *Concepts in Biological Oceanography: An Interdisciplinary Primer*. Oxford University Press, 1993.
[52] Ian D. Lunt and Peter G. Spooner. Using historical ecology to understand patterns of biodiversity in fragmented agricultural landscapes. *Journal of Biogeography*, 32:1859–1873, 2005.
[53] L. Wanga, B. L. Walkera, S. Iannacconeb, D. Bhatta, P.J. Kennedya, and W.T. Tse. Bistable switches control memory and plasticity in cellular differentiation. *PNAS U S A*, 106(16):6638–6643, 2009.
[54] K. Lai, M. J. Robertson, and D. V. Schaffer. The sonic hedgehog signaling system as a bistable genetic switch. *Biophys J*, 86:2748–2757, 2004.
[55] S. Graziani, P. Silar, and M.-J. Daboussi. Bistability and hysteresis of the 'secteur' differentiation are controlled by a two-gene locus in nectria haematococca. *BMC Biology*, 2(18):1–19, 2004.
[56] M. Thattai and B. Shraiman. Metabolic switching in the sugar phosphotransferase system of escherichia coli. *Biophys J*, 85:744–754, 2003.
[57] D. M. Wolf, L. Fontaine-Bodin, I. Bischofs, G. Price, J. Keasling, and A. P. Arkin. Memory in microbes: quantifying history-dependent behaviour in a bacterium. *PLoS ONE*, 3(2):e1700, 2008.
[58] W. K. Smits, O. P. Kuipers, and J. W. Veening. Phenotypic variation in bacteria: the role of feedback regulation. *Nat Rev Microbiol*, 4:259–271, 2006.
[59] H. Maamar, A. Raj, and D. Dubnau. Noise in gene expression determines cell fate in bacillus subtilis. *Science*, 317:526–529, 2007.

CRM Preprint Series number 1215

[60] T. S. Ham, S. K. Lee, J. D. Keasling, and A. P. Arkin. Design and construction of a double inversion recombination switch for heritable sequential genetic memory. *PLoS ONE*, 3(7):e2815, 2008.
[61] D. Dubnau and R. Losick. Bistability in bacteria. *Mol Microbiol*, 61:564–572, 2006.
[62] M. Delbrück. Translation of discussion following a paper by sonneborn, t. m. and beale, g. h. *Unité Biologiques Douées de Continuité Génétique. Editions du Centre National de la Recherche Scientifique, Paris*, pages 33–35, 1949.
[63] A. Novick and M. Weiner. Enzyme induction as an all-or-none phenomenon. *Proc Natl Acad Sci USA*, 43(7):553–566, 1957.
[64] M. Cohn and K. Horibata. Inhibition by glucose of the induced synthesis of the beta-galactoside-enzyme system of escherichia coli. *Analysis of maintenance. J Bacteriol*, 78:601–612, 1959.
[65] M. Cohn and K. Horibata. Analysis of the differentiation and of the heterogeneity within a population of eschericia coli undergoing induced beta- galactosidase synthesis. *J Bacteriol*, 78:613–623, 1959.
[66] M. Cohn and K. Horibata. Physiology of the inhibition by glucose of the induced synthesis of the beta-galactoside-enzyme system of escherichia coli. *J Bacteriol*, 78:624–635, 1959.
[67] Ö. Winge and C. Roberts. Inheritance of enzymatic characters in yeast and the phenomenon of long term adaptation. *Comp rend trav Lab, Carlsberg. Ser physiol*, 24:263–315, 1948.
[68] E. Kussell and S. Lieber. Phenotypic diversity, population growth, and information in fluctuating environments. *Science*, 309:2075–2078, 2005.
[69] H. J. E. Beaumont, J. Gallie, C. Kost, G. C. Ferguson, and P. B. Rainey. Experimental evolution of bet hedging. *Nature*, 462:90–93, 2009.
[70] M. Acar, J. MettetalT, and A. van Oudenaarden. Stochastic switching as a survival strategy in fluctuating environments. *Nature Genetics*, 40(4):471–475, 2008.
[71] M. Acar, A. Becskei, and A. vanO udenaarden. Enhancement of celluar memory by reducing stochatsic transitions. *Nature*, 435:228–232, 2005.
[72] B. B. Kaufmann, Q. Yang, J. T. Mettetal, and A. van Oudenaarden. Heritable stochastic switching revealedby single-cell genealogy. *PLoS Biol*, 5(9):e239, 2007.
[73] M. Thattai and A van Oudenaarden. Stochastic gene expression in fluctuating environments. *Genetics*, 167:523–530, 2004.
[74] G. Friedman, S. McCarthy, and D. Rachinskii. Hysteresis can grant fitness in stochastically varying environment. *PLOS ONE*, 9(7):e103241, 2014.
[75] H. N. Lim and A. van Oudenaarden. A multistep epigenetic switch enables the stable inheritance of dna methylation states. *Nat Genet*, 39:269–725, 2007.
[76] C. V. Rao, D. M. Wolf, and A. P. Arkin. Control, exploitation and tolerance of intracellular noise. *Nature*, 420:231–237, 2002.

A. Pimenov
Weierstrass Institute
Mohrenstrasse 39
D-10117 Berlin, Germany
E-mail address: alexander.pimenov@wias-berlin.de

T.C. Kelly
Department of Biology Earth and Environmental Science
University College Cork, Ireland
E-mail address: t.kelly@ucc.ie

CRM Preprint Series number 1215

A. Korobeinikov
Centre de Recerca Matemàtica
Campus de Bellaterra, Edifici C
08193 Barcelona, Spain
and
Departament de Matemàtiques
Universitat Autònoma de Barcelona
Campus de Bellaterra, Edifici C
08193 Barcelona, Spain
E-mail address: akorobeinikov@crm.cat

M.J.A. O'Callaghan
Department of Applied Mathematics
University College Cork
Ireland
E-mail address: mja.ocallaghan@ucc.ie

D. Rachinskii
Department of Mathematical Sciences
The University of Texas at Dallas
800 W. Campbell Road, Richardson
Texas 75080, USA
E-mail address: dmitry.rachinskiy@utdallas.edu
phone: +1 972 883 6697
Corresponding author

CRM Preprint Series number 1215

CRM
CENTRE DE RECERCA MATEMÀTICA
Facultat de Ciències, UAB
08193 Bellaterra
Barcelona, Spain
www.crm.cat